
Learning by serialization

Anonymous Author(s)

Affiliation

Address

email

Abstract

1 Complex structures such as sets, trees or graphs are typical in machine learning.
2 Tailoring learning algorithms for every structure requires an effort that may be
3 saved by defining a generic learning procedure adaptive to any complex structure.
4 In this paper, we propose to map any complex structure onto a generic form, called
5 serialization, over which any sequence density estimator may be applied. The
6 learned density may then be transferred back onto the space of original structures.
7 In order for learning to be exposed to the structural particularities of the original
8 structures, care must be taken that the serializations reflect and describe accurately
9 their properties. Enumerating all serializations is infeasible. We propose an
10 effective way to sample representative serializations from this complete set while
11 retaining their statistics in the complete set. Our method is competitive or better
12 than state of the art learning algorithms specifically designed for different structures.
13 In addition, since serialization involves sampling from a combinatorial process
14 it provides considerable protection from overfitting, clearly demonstrated over
15 a number of experiments. This opens the door to trying ever more complex
16 architectures without the curse of overfitting.

17 1 Introduction

18 Many learning problems are defined over complex instance structures, e.g. learning instances can be
19 sets, trees, sequences etc. One typical approach to such problems is the so-called propositionalisation,
20 Lavrac & Dzeroski (2001), in which one maps such complex learning instances to vectorial representa-
21 tions, potentially losing discriminative information along the way. Yet another approach is to develop
22 learning algorithms tailored to the representation particularities of any given problem, preserving in
23 that manner all learning information, at the cost of significant conceptual and development effort.

24 Instead, we propose to decouple learning from the structural specificities of the learning instances.
25 To do so, we define an informed, randomized, mapping from any given complex-structured instance
26 onto *multiple* and *equivalent* sequences. We then learn over the space of sequences and map back
27 the result of the learning onto the space of original instance structures. When mapping a complex
28 instance structure onto a sequence, we must retain the specificity of the original structure and preserve
29 its properties in order to guarantee a revertible mapping. We do so by carrying over the mapping a set
30 of constraints and properties of the original instance structures and integrating them into the learning
31 process via the appropriate design of learning instances.

32 Our framework has a number of advantages. It opens a sound and systematic way to perform
33 learning over arbitrary complex instance structures. Any learning algorithm defined over sequences
34 is directly usable, making it very easy to benefit from and apply all the latest advances on learning
35 over sequences, by simply plugging it in our framework. Finally, the fact that we map the instances
36 to multiple and equivalent sequences over which we learn brings, as we will demonstrate, significant
37 advantages when it comes to overfitting avoidance. We focus on generative modeling over complex
38 structures, since it can be used to solve many machine learning tasks including unsupervised learning
39 and supervised learning.

2 Related Work

The recent surge on generative modeling has seen the development of generative methods that can learn, implicit or explicit, distributions over complex instances and sample from them. We have applications of generative modeling in problems where the learning instances are two dimensional structures, e.g. images (two-dimensional structures), (Balcan & Weinberger, 2016; Goodfellow et al., 2014; Sohn et al., 2015; Rezende et al., 2014; Kingma & Welling, 2013), sequences for speech, (van den Oord et al., 2016), text (Graves, 2013), translation (Sutskever et al., 2014b), and graphs, e.g. drug modeling, (Gómez-Bombarelli et al., 2016).

Of more interest to our work are generative models for structures such as sets (Vinyals et al., 2015; Zaheer et al., 2017) and trees (Alvarez-Melis & Jaakkola, 2016; Zhang et al., 2016; Dong & Lapata, 2016; Liu et al., 2011; Zhou et al., 2017). Such models incorporate the specificities of the original instance structure on how they factorize the generative distribution to a product of conditionals. The factorization controls the dependencies between the components of a given learning instance, ensuring that the inherent properties of the original instance structure are preserved. Examples of structural properties that can be expressed via the factorization of the conditionals are order independence and invariance to transformations of the conditioned variable (Oliva et al., 2017; Uria et al., 2016). These properties are used to express invariances of specific complex structures such as the invariance to re-ordering of conditioning for sets (Vinyals et al., 2015; Zaheer et al., 2017), invariance to re-ordering of siblings for trees and invariance to relabeling of nodes for graphs.

In our approach, we take a constructive modeling of the mapped sequences (*serializations*) and transfer the invariance properties of the original complex structures onto constraints in the model for constructing these serializations. We model structure invariance via states representing the relevant information that the system has acquired at a given step of the generative process. The inherent properties of the original structure are thus expressed by which partial serializations are represented by the same state or not. For example, the invariance against re-ordering is expressed by the fact that building a given sub-structure by following two different orderings leads to the same state. The specific representation of a state is domain-specific and also allows to incorporate further information about the inherent properties of the original structures.

The Grammar Variational Autoencoder (Kusner et al., 2017) learns generative models over arbitrary complex structures. It describes structures by a context-free grammar and then uses a parser to create a sequence of production rules on which it learns a standard Variational Autoencoder. It reconstructs the original instance by predicting the sequence of production rules. It can be viewed as a special case of our framework since a context-free grammar can be transformed into a state-transition function with a state containing a representation of what has been parsed so far, and transitions consisting of the application of the different production rules. Our framework makes explicit the notion of a *state* and uses it to enforce constraints on the probabilities of occurrences of training serializations.

3 Method

We are given a space \mathbb{X} of complex structured learning instances, equipped with an unknown probability distribution $P_{\mathbb{X}}$, of which we want to learn a model, $P_{\mathbb{X},\phi}$ using a training set $\mathcal{X} = \{x_1, \dots, x_n | x_i \in \mathbb{X}\}$ of n instances sampled i.i.d from $P_{\mathbb{X}}$ (ϕ is the set of model parameters). We measure the quality of the learned distribution with the likelihood on the training/testing data.

3.1 The space of serializations

To learn the probability distribution over the space of the original complex structures \mathbb{X} , we first map each structured instance $x \in \mathbb{X}$ onto a sequence $a \in \mathbb{A}$, where \mathbb{A} is the space of sequences of finite but unknown length over some finite lexicon \mathbb{B} ; the latter is given by the domain of the problem. We denote by $\mathcal{A} \subseteq \mathbb{A}$ the set of sequences generated by taking the maps of all training instances $x \in \mathcal{X}$. We then learn a probability distribution, $P_{\mathbb{A},\phi}$, over \mathbb{A} , training an RNN on \mathcal{A} . We use the learned distribution to construct $P_{\mathbb{X},\phi}$ in the original space. We call our proposal S-RNN (as Structural RNN) since it embarks extra structural information into a RNN-based learning of sequences.

Since \mathcal{A} is the only access the learner has to our specific domain problem and its constraints, it is critical that we provide the learner with quality information. To carry over the constraints from \mathbb{X} to \mathbb{A} without explicitly constraining the learner, we map every $x \in \mathcal{X}$ onto multiple sequences a_j , *serializations* of x , exhibiting the invariance properties of the original structure x . Hence,

93 $a_j = [a_j^1, a_j^2, \dots, a_j^m] \in \mathbb{A}$, its elements are $a_j^i \in \mathbb{B}$, and m is the length of a_j . We discuss later the
 94 serializations and the *serialization algorithm* we use. For now, we simply note that the serialization
 95 algorithm parses the complex structure and produces in a sequential manner a serialization a_j . For
 96 example, a set $x = \{A, B, C\}$ can be mapped onto any of its multiple serializations, say $a_1 = [A, B, C]$,
 97 $a_2 = [A, C, B]$, $a_3 = [B, C, A]$, etc, thus exhibiting order invariance. A *partial serialization* of x is a
 98 subsequence $a_j^{[1:d]} = [a_j^1, a_j^2, \dots, a_j^d]$, $d \leq m$.

99 Invariance properties on x will be mapped onto invariance to local or global reordering in a_j (eg
 100 “swapping elements in the serialization of a set doesn’t matter”) and/or conditioning the occurrence of
 101 subsequences in a_j to its preceding subsequences (eg “if ‘A’ has occurred in the partial serialization,
 102 it will not appear anymore since elements occur only once within a set”). Ideally, the training set
 103 \mathcal{A} should list all possible serializations of x to exhibit the invariance properties via examples to the
 104 learner. Since in general this is neither possible nor desirable it is important to account for the choices
 105 our procedure makes over all possible serializations. Making efficient this implicit normalization is
 106 one of the contributions of our proposal.

107 The serialization algorithm defines a mapping from an original instance x onto a stochastic process
 108 whose sampled realizations will create the serializations a_j , feeding \mathcal{A} . This mapping (serialization
 109 algorithm) is part of domain knowledge and is always done so as to be revertible, i.e guarantees that a
 110 serialization a_j generated from instance x reconstructs/de-serializes to x and only x . In the next
 111 section, we first discuss the mapping from \mathbb{X} to \mathbb{A} and how from this we extract a density on \mathbb{X} . In
 112 section 3.3, we address the construction of \mathcal{A} in detail.

113 3.2 Serialization with no structural constraints

114 We assume that \mathbb{A} is a probability space equipped with a distribution $P_{\mathbb{A}}$, of which an estimate $P_{\mathbb{A},\phi}$
 115 we learn by applying an RNN on set \mathcal{A} . Here, we detail how we generate a distribution $P_{\mathbb{X},\phi}$ from
 116 $P_{\mathbb{A},\phi}$ and our abstract model for maintaining the creation of a relevant training set \mathcal{A} .

117 We assume \mathbb{X} to be measurable and define the random variable $X : \mathbb{A} \rightarrow \mathbb{X}$. We install a probability
 118 distribution $P_{\mathbb{X},\phi}$ over the original space \mathbb{X} by pushing forward the distribution $P_{\mathbb{A},\phi}$ learned in the
 119 serialization space \mathbb{A} along X . The r.v. X classically allows us to compute probabilities over \mathbb{X} by:

$$P_{\mathbb{X},\phi}(x) \triangleq P_{\mathbb{A},\phi}(\{a_j \in \mathbb{A} | X(a_j) = x\}) = P_{\mathbb{A},\phi}(X^{-1}(x)) = \sum_{a \in X^{-1}(x)} P_{\mathbb{A},\phi}(a)$$

120 Following our earlier description, X is the de-serialization procedure mapping a serialization a_j
 121 to the original data $X(a_j) = x$. In turn, X^{-1} , as a serialization process, represents the stochastic
 122 process sampling from the set of all possible serializations of x , $X^{-1}(x) = \{a_j \in \mathbb{A} | X(a_j) = x\}$.
 123 Serializing via a particular serialization algorithm X^{-1} and therefore choosing a subset of all possible
 124 serializations creates a bias in the representation of x within \mathcal{A} that we need to account for to maintain
 125 accurate learning. We discuss here how this may be done by adding an extra abstract structure on
 126 the space \mathbb{A} , reflecting properties of the sequences in \mathbb{A} and thus enabling the description of our
 127 serialization algorithm and measure its limitations in covering the space of all possible serializations
 128 of \mathcal{X} with \mathcal{A} .

129 We define a random variable $O : \mathbb{A} \mapsto \mathbb{O}$, where \mathbb{O} is a measurable space of *properties*. Using O^{-1} ,
 130 we map these properties onto \mathbb{A} . An illustrative example of such properties on sequences is “elements
 131 of the sequence are in alphabetical order”. Events o are properties that apply to sequences in \mathbb{A} in
 132 general and will help characterize serializations as follows. A sequence $a_j \in \mathbb{A}$ may therefore be
 133 a serialization of $x \in \mathbb{X}$ (ie $a_j \in X^{-1}(x)$) and/or bear property $o \in \mathbb{O}$ (ie $a_j \in O^{-1}(o)$). Thus,
 134 given an original instance x and a property $o \in \mathbb{O}$ on sequences, the set of serializations of x bearing
 135 property o is $O^{-1}(o) \cap X^{-1}(x)$.

136 We then adapt equation 1 to integrate knowledge on the choice of the subset of all possible serializa-
 137 tions, controlled by variable o :

$$P_{\mathbb{X},\phi}(x) = \frac{P(o, x)}{P(o|x)} \quad \forall o \in \mathbb{O} \quad (1)$$

138 The numerator is computed using the distribution learned on the \mathbb{A} space ($P_{\mathbb{A},\phi}$), and is given by:

$$P(o, x) \triangleq \sum_{a \in X^{-1}(x) \cap O^{-1}(o)} P_{\mathbb{A},\phi}(a) \quad (2)$$

By structuring \mathbb{A} , O therefore helps the counting of serializations by grouping them according to their properties o . Since in practice, we can enumerate and count all possible serializations of x produced by the serialization algorithm, we can consider $X^{-1}(x)$ (and hence its subset $X^{-1}(x) \cap O^{-1}(o)$) countable. Further, if we consider o as being a property of any given serialization, X^{-1} will produce a limited number of such serializations, which makes the numerator easy to compute, at the cost of normalizing properly.

The denominator here models the normalizer which accounts for the limitation of our serialization algorithm in terms of its properties. It is directly related to the way the serialization algorithm X^{-1} , as a stochastic process produces \mathcal{A} , which we describe now.

We denote by \mathbb{F} the set of events of \mathbb{A} . We see the stochastic process installed by X^{-1} as a sampling strategy defined by an arbitrary measure $\mu : \mathbb{F} \mapsto \mathbb{R}_{>0}$. Hence, a run of the serialization algorithm is computing a set of serializations $X^{-1}(x)$ and picks one according to the weight measure μ for feeding the training set \mathcal{A} . μ therefore comes as a support to the calculation of our normalizer $P(o|x)$ as

$$P(o|x) \triangleq \frac{\mu(X^{-1}(x) \cap O^{-1}(o))}{\mu(X^{-1}(x))} \quad (3)$$

This abstract modeling will be exploited and modified in the next section to enforce constraints on the serializations as a reflection of the invariance properties of the original structure.

Equations 1 and 2 show that, to compute $P_{\mathbb{X},\phi}(x)$, we need $P_{\mathbb{A},\phi}(a)$. We fit $P_{\mathbb{A},\phi}$ by maximum likelihood on \mathcal{A} or equivalently minimizing the KL divergence between $P_{\mathbb{A}}$ and $P_{\mathbb{A},\phi}$: $P_{\mathbb{A},\phi} \triangleq \arg \min_{\tilde{P}} \text{KL}(P_{\mathbb{A}} || \tilde{P})$. Hence, classically, given representative enough training data \mathcal{A} and appropriate regularization (ie a flexible enough model family for $P_{\mathbb{A},\phi}$), the learned distribution will be close to the real $P_{\mathbb{A}}$.

3.3 Serializations with structural constraints

The serializations considered so far are placed into \mathcal{A} on the basis of their global occurrences (ie as complete serializations) and sampling distribution μ . Hence, μ should be adapted so as to compensate for the bias in the sampling. One practical way to adapt μ is to inform the distribution on the internals of the serializations sampled.

Returning to our simple set example, since a set is invariant to ordering, it is clear that serializations $a_3 = [\text{B}, \text{C}, \text{A}]$ and $a_4 = [\text{C}, \text{B}, \text{A}]$ are equivalent, so are their partial serializations $a_3^{[1:2]} = [\text{B}, \text{C}]$ and $a_4^{[1:2]} = [\text{C}, \text{B}]$. We can explicitly model this equivalence by constraining the conditional probability of the next element given equivalent partial serializations to be the same, i.e. $P_{\mathbb{A},\phi}(a_3^3 = b | a_3^{[1:2]}) = P_{\mathbb{A},\phi}(a_4^3 = b | a_4^{[1:2]}) \quad \forall b \in \mathbb{B} = \{\text{A}, \text{B}, \text{C}, \text{D}, \text{E}\}$. More generally, given two serializations a_i and a_j , the t -length partial serializations of which, are equivalent we require that:

$$P(a_i^{t+1} = b | a_i^{[1:t]}) = P(a_j^{t+1} = b | a_j^{[1:t]}) \quad \forall b \in \mathbb{B} \quad (4)$$

Equation 4 transfers the structural invariances of the original instances $x \in \mathbb{X}$ to the serialized structures $a \in \mathbb{A}$ produced from them. The constraints are enforced by characterizing equivalent partial sequences of a_i and a_j and ensuring that the probability distribution of the next element is the same. Formally, we define a state space \mathbb{S} and map sequences \mathbb{A} to the state space \mathbb{S} so that equivalent partial sequences have the same state. \mathbb{S} is equipped with a transition function $f : \mathbb{S} \times \mathbb{B} \rightarrow \mathbb{S}$ governing the construction of a sequence via its equivalent states. Hence, a serialization $[a^1, \dots, a^t, \dots, a^T]$ is represented by the sequence of states $s^0, \dots, s^t, \dots, s^T$ produced by the recurrence:

$$s^{t+1} = f(s^t, a^{t+1}) \quad \forall 0 \leq t < T \quad (5)$$

where s^0 is an initial state representing an empty sequence in \mathbb{A} , and therefore an object in \mathbb{X} (eg an graph with no node or an empty set). At any step, a partial sequence $a^{[1:t]} = [a^1, \dots, a^t]$ is represented by state s^t . Hence,

$$P(a^{[t+1:T]} | a^{[1:t]}) = P(a^{[t+1:T]} | s^t) \quad (6)$$

By combining equations 5 and 6, and imposing at step t that the state s_i^t of partial sequence a_i is the same as the state s_j^t of partial sequence a_j , if the two partial sequences are equivalent, we model the

183 equivalence relationship in equation 4 in the state space.

$$P(a_i^{t+1} = b | s_i^t) = P(a_j^{t+1} = b | s_j^t) \quad \forall b \in \mathbb{B} \quad (7)$$

184 Modeling with states enables the factorization of structural constraints on the serializations. Such
 185 constraints create correlations between (sub-)serializations and prevent us from sampling serializations
 186 at once, as described earlier. Even different instances x may share substructures and thus share
 187 equivalent partial serializations. We therefore also need to impose the constraints between equivalent
 188 partial serializations across different instances. To do so we sample at the level of the serialization
 189 element. We adapt our sampling measure μ to reflect these equivalence constraints. In other words,
 190 we adapt μ to express how the next element a^{t+1} is sampled from \mathbb{B} with respect to the state $s^t \in \mathbb{S}$.
 191 We redefine the measure as $\mu : \mathbb{S} \times \mathbb{B} \rightarrow \mathbb{R}_{>0}$ to provide a measure over the joint set of states (s^t)
 192 and the lexicon from where a^{t+1} will be sampled.

193 In practice, defining an appropriate μ is difficult but this guides to an interesting algorithmic solution.
 194 We summarize in Algorithm 1 a procedure to efficiently sample a serialization, focusing on the struc-
 195 tural constraints and compensating for the bias coming from the specificity of the base serialization
 196 algorithm X^{-1} .

197 Given a base set of serializations $A_{\text{all}} = X^{-1}(x)$, the procedure samples, element by element, a
 198 serialization guaranteed to come from the base set according to the statistics of the base set and μ . At
 199 each time step t , the procedure stores in \mathcal{L} all elements a_j^t as plausible next elements for the currently
 200 reconstructed sequence $a_{\text{sample}}^{[1:t-1]}$. The next element a^{next} is then sampled from \mathcal{L} using μ and s and
 201 concatenated to $a_{\text{sample}}^{[1:t-1]}$ (ie $a_{\text{sample}}^t = a^{\text{next}}$). In order to preserve the consistency of the serialization
 202 sampled, all serializations in A_{all} not having element a^{next} as t th element are removed from A_{all} .

203 Note that for example, in the simple case of sets of size n , this decimation (equivalent to saying
 204 that every element may appears once only and at any position) will lead to every serialization (with
 205 no restriction on their property) having a probability of $\frac{1}{n!}$, which is consistent with the reality.
 206 Interestingly, thanks to this last step, since \mathcal{L} samples the next element from $X^{-1}(x)$, μ is not
 207 required to bring more information and may be taken as uniform. States are then updated following
 208 equation 5. This procedure therefore makes very efficient the creation of an unbiased training set \mathcal{A}
 209 informing the learner about the structural constraints within \mathbb{X} .

210 3.4 Regularized learning

211 Having constructed a valid training set \mathcal{A} transferring our domain knowledge onto \mathbb{A} , we use a RNN
 212 to learn $P_{\mathbb{A}, \phi}$. We can support the RNN in its learning by way of a regularizer constructed around the
 213 constraints of our domain. To this end, we use equation 7 again and create a binary sparse matrix
 214 (C_{jk}^t) ($j, k = 1 \dots |\mathcal{A}|, t = 1 \dots T$) storing state equivalences with the serializations $a_j \in \mathcal{A}$ (ie
 215 $C_{jk}^t = 1$ iff $s_j^t = s_k^t$).

216 Let $h_t \in \mathbb{R}^H$ be the H -dimensional hidden state of the RNN. The probabilistic model of an RNN is
 217 given by:

$$h^0 = 0 \quad ; \quad h^t = \sigma(W_{hh}h^{t-1} + W_{hi}a^t) \quad ; \quad P(a^1, \dots, a^T) = \prod_{t=1}^T P_{\theta}(a^t | h^{t-1}) \quad (8)$$

218 where W_{hh} is the hidden-to-hidden weight matrix, W_{hi} the input-to-hidden weight matrix and P_{θ} is
 219 a distribution with parameters θ .

220 The loss of our learning objective is given by:

$$L = - \sum_{j=1}^{|\mathcal{A}|} \sum_{t=1}^T \ln(P_{\theta}(a_j^{t+1} | h_j^t)) + \lambda \sum_{k,l,t} C_{kl}^t \left\| \frac{h_k^t}{\|h_k^t\|} - \frac{h_l^t}{\|h_l^t\|} \right\| \quad (9)$$

221 We regularize with the normalized hidden states to avoid that the regularizer has any effect on the
 222 norm of the hidden state. Note, that C is very sparse so that the regularizer may be computed
 223 efficiently using sparse structures for space \mathbb{S} .

3.5 Recovering the density on the original structures

Given a trained model we want to compute the probability of an instance x_{test} and obtain $P_{\mathbb{X},\phi}(x_{\text{test}})$. We rely on equations 1, 2 and 3. Additionally, in practice we know what serialization algorithm we use, and also know its properties (ie the properties of the serializations it produces). We use this knowledge to compute $P(o|x_{\text{test}})$ without generating all serializations in $X^{-1}(x_{\text{test}})$ and also use the same algorithmic enumeration of serializations as proposed in Algorithm 1 to estimate their specific probability of occurrence.

In this context, we are able to count the possible outputs of our serialization algorithm and get $|X^{-1}|$. For sets of size n for example, due to invariance against element reordering, we get $|X^{-1}| = n!$, so that every set serialization is equilikely with probability $\frac{1}{n!}$. For more complex structures, we can, for example, keep track of the number of (uniform) random choices we make (eg in the exploration of a tree) and obtain similar statistics.

We also know the *properties* of our algorithm. Hence, we may either consider a property o_j leading to $|X^{-1}(x_{\text{test}}) \cap O^{-1}(o_j)| = 1$ (eg o_j = “elements in alphabetical order”) or, at least we can enumerate the number of serializations with property o_j we get. In the context of a selection of serialization of x_{test} via property o_j , not every serialization is equilikely. As discussed in section 3.3 and similarly to what is proposed in Algorithm 1, we normalize the probability of occurrence of a given serialization via its construction using our state space. As a result again, μ needs not to be informative in the general case and can simply be chosen as uniform

Hence, given one serialization a_j of x_{test} with property o_j , we access its learned probability $P_{\mathbb{A},\phi}(a_j)$. We can extract the number of serializations a bearing the same property o_j and therefore easily compute $P(o_j|x_{\text{test}})$. Similarly, by normalizing serializations for their probability of occurrence, we get $P(o_j|x_{\text{test}})$ and therefore are able to compute an estimate of $P_{\mathbb{X},\phi}(x_{\text{test}})$ via a_j . Generating m equivalent serializations of x_{test} by using m times algorithm 1 to obtain (a_j) with $j = 1, \dots, m$ (each bearing property o_j), we can improve the accuracy of the estimate by taking the expectation so we finally get:

$$P(X = x_{\text{test}}) \approx \frac{1}{m} \sum_{j=1}^m \frac{\sum_{a \in X^{-1}(x_{\text{test}}) \cap O^{-1}(o_j)} P_{\mathbb{A},\phi}(a)}{P(O = o_j|X = x_{\text{test}})} \quad (10)$$

4 Experiments

We explore the performance of S-RNN on a set of learning problems where learning instances have diverse structures; we work on multivariate sequences/time-series, trees, and standard propositional problems. Our goal is to explore the performance and behaviour of S-RNN over a variety of structures and demonstrate that it can achieve performance that are comparable to different state of the art systems that have been specifically tailored to each one of these structures.

Multivariate dynamical systems datasets We explore the performance of S-RNN on two datasets, artificial and real world. Both are essentially multivariate dynamical systems. We generate the artificial dataset using a known dynamical system. The real world (gait) dataset contains recordings of gait trajectories of people with pathological gait. Both datasets have a similar structure and differ only by their dimensionalities. In particular each training instance consists of two components: $\mathbf{x} \in \mathbb{R}^d$, which we call input, and $\mathbf{Y} \in \mathbb{R}^{k \times l}$ which we call output; with the latter being a probabilistic function of the former. The \mathbf{Y} matrix contains a k -dimensional dynamical system uniformly sampled at l time points. We address a supervised task in which the goal is to learn to predict \mathbf{Y} given \mathbf{x} , and an unsupervised task in which we seek to learn $P(\mathbf{Y})$ and sample from it. In both we measure performance with the negative log-likelihood. In the appendix, section B.1, we give a complete description of the datasets, the serialisation procedure, the learning architecture, the baseline models, and the evaluation procedure. We took special care to compare against baseline modes that have equivalent learning power as the ones we use with S-RNN.

In the artificial dynamical system we only experiment with the supervised setting. S-RNN learns the joint distribution $P(\mathbf{x}, \mathbf{Y})$ and uses that to predict the most probable class, i.e. the one that maximizes the conditional likelihood $P(\mathbf{Y}|\mathbf{x})$. We start by exploring the learning behavior of S-RNN. In the left graph of figure 1 we give the evolution of the conditional negative log-likelihood on the validation set as a function of the training iterations (number of mini-batches seen) for S-RNN with and without regularisation and the RNN baseline. The most striking observation from that figure is that S-RNN never overfits. The baseline we used, RNN, starts overfitting after around 5k mini-batch

S-RNN	S-RNN $\lambda = 10^2$	S-RNN $\lambda = 10^4$	RNN
-107	-103	-57	-41

Table 1: Test set negative log likelihood, artificial dynamical system, supervised setting. Bold indicate performances that are significantly better than the non-bold.

iterations, time at which it will have seen every training instance on average 160 times. S-RNN practically will never see an instance twice due the combinatorial complexity of the serialisation generation and can keep on training practically forever with no overfitting. This behavior is even more clear in the middle graph of the same figure where we plot the train/test set evolution of the conditional likelihood. We give the performance results (negative log likelihood) in table 1. S-RNN with no regularisation achieves the best result, far better and significantly better than the baseline; we controlled the statistical significance using a t-test. Mildly regularising S-RNN does not seem to bring any performance gain, while strong regularisation harms. The fact that regularisation does not bring any effect can be explained by the fact that the algorithm never sees twice the same serialisation. In the appendix we provide a more detailed discussion of the above; in addition we show figures of the predicted \mathbf{Y} component (figure 3, section B.1) in order to inspect the visual quality of the results.

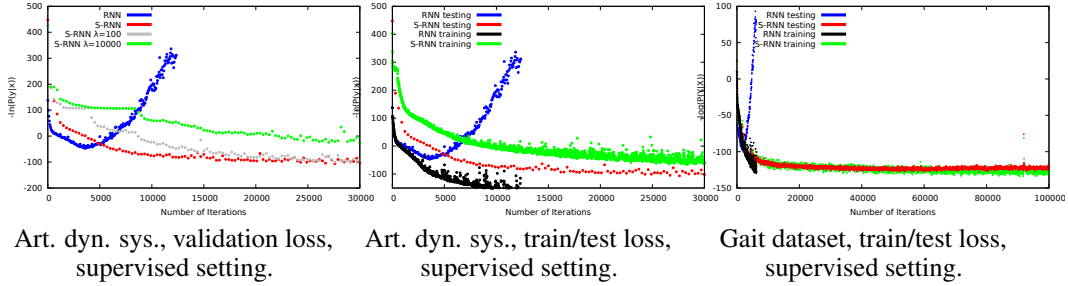


Figure 1: Overfitting behavior on the dynamical system problems, supervised setting. Left: Conditional negative log likelihood on the validation set as a function of training iterations, artificial dynamical system, includes different regularisation levels for S-RNN. Middle: Same as the left but on train/test sets. Right: Same as the middle but on the Gait dataset.

We experiment with the gait dataset both in the unsupervised setting where the goal is to learn a model of $P(\mathbf{Y})$ and being able to sample from it, and in the supervised setting as above. In the left side of table 2 we give the results for the unsupervised case in terms of the negative log-likelihood on the test set, for different dimensionalities (k) of the sequence part \mathbf{Y} . S-RNN achieves a performance which is always considerably better than the RNN baseline. In the appendix (figure 4) we also give examples of samples drawn from S-RNN and the baseline as well as real samples.

In the supervised setting we experimented with one and two dimensional sequences (corresponding to one and two joint angles respectively). The performance results are in the right side of table 2. On the 1D sequences S-RNN is significantly worse compared to RNN. The situation is reversed when we consider two angles. We hypothesize that the low performance in the one-angle setting is because most of the network representation power is consumed in learning and expressing correlations between the input features. With two angles we are able to learn and express correlations between the angles themselves, thus the better performance. We again check the behavior of S-RNN on the two angle dataset with respect to overfitting by visualising the evolution of the negative log likelihood in the training and testing set right graph of figure 1. As it was also the case with the artificial dataset we never observe a divergence between the learning performance on the training and the testing set; note that here we let S-RNN to train for 100k iterations and we never observe a divergence between the train and test loss. In the appendix we provide additional results visualising the quality of samples produced by the generative model, as well as from the supervised model, and also explore the sensitivity of the predictions to the serialisation of the inputs.

Tree datasets We experiment with S-RNN on two different learning tasks involving instances that are represented by trees. We consider ordered and unordered trees. The first task is an unordered tree prediction task in which the goal is to generate a tree given its textual description. Thus here a learning instance is a (\mathbf{x}, \mathbf{Y}) , pair where the predictive component \mathbf{x} is a sequence and the target \mathbf{Y} is a tree. The second task is a regression task where the goal is to predict a scalar given a tree, i.e. learning instances are now of the form (\mathbf{X}, y) , where \mathbf{X} is a tree and $y \in \mathbb{R}$. For the tree prediction

# of Angles (k)	S-RNN	RNN
	mean	mean
2	-6.8	7.3
4	-66	-14
8	-32	83.3

# Angles (k)	S-RNN	RNN
	mean	mean
1	-47	-53
2	-125	-97

Table 2: Test set negative log likelihood on the unsupervised (left) and supervised (right) gait problems. Bold indicates performances that are significantly better than the non-bold.

task we compare against the results of the DRNN method introduced in Alvarez-Melis & Jaakkola (2016) (from where we took the dataset and the evaluation protocol). For the regression task we compare against the results of two Tree Echo State Network variants, TreeESN-R and TreeESN-M (Gallicchio & Micheli (2013)), specifically developed for trees. In section B.4 of the appendix we provide detailed descriptions of the datasets, the serialisation applied on the tree structures, the learning architecture, the evaluation protocol and of the respective baselines.

The tree prediction task is evaluated as a retrieval task, where precision, recall and F1 score are used to evaluate the quality of retrieval of the tree nodes and edges. We give the results in table 3. S-RNN outperforms by an important margin the baseline for all measures except recall. In table 4 we give the predictive error results for the regression task, here we consider both ordered and unordered trees. The two variants of S-RNN, i.e. trained on ordered and unordered trees, give better results than TreeESN-R, while they perform worse than TreeESN-M. We also explored the overfitting behavior of S-RNN by tracking the evolution of the loss in the training/validation/test sets (graphs in figure 6 of the appendix). Again there is hardly any divergence between the three losses even after very large number of training iterations, with the exception of the ordered trees version, which due to its nature does not allow for multiple serialisations (more details for the latter in the appendix, section B.4.2).

Method	Node F1	Node precision	Node Recall	Edge F1	Edge Precision	Edge Recall
S-RNN	88.95%	87.82%	90.79%	83.43%	82.22%	85.47%
DRNN	74.51%	59.37%	100%	65.86%	49.10%	100%

Table 3: Performance results for the tree prediction task.

Propositional datasets Here we experiment on a set of standard classification datasets taken from UCI. We serialise a vectorial instance as a sequence which we generate by randomly sampling features without replacement. We compare against a Multi Layer Perceptron (MLP) which has an equivalent architecture to our S-RNN model. As before a detailed description of the experiments and the results can be found in the respective section (B.5) of the appendix. The accuracy of the two methods is very similar over all the datasets (see appendix, table 10). However what is striking is the resistance to overfitting that S-RNN exhibits with respect to the length of training when compared to the standard MLP. With the exception of the iris dataset, which probably due to its small number of features that does not allow for the randomization effect to kick in, the loss values in the training/validation/test sets are very similar for S-RNN, i.e. there is hardly any divergence. MLP, in all datasets except iris exhibits considerable divergence between the different losses, which takes place rather early in the learning. These empirical results confirm what we already observed in the previous data structures, i.e. that the randomization inherent in the serialisation process brings a robust protection against overfitting, allowing training to continue for considerably longer horizons.

5 Conclusion

We have presented S-RNN, a framework for performing density estimation over arbitrary complex data structures. S-RNN achieves state of the art performance on a number of different structures, comparable or better than the performance of methods specifically developed for these structures. Our genericity relies on the existence of a serialization/de-serialization procedure for the type of data in question. The knowledge and control of the serialization operations allow us to write principles for normalization, enabling the effective transfer of structural properties of the original data onto generic sequences an RNN will learn. The combinatorial nature of the intermediate serialization operation generates a potentially unlimited set of training samples. The diversity and uniqueness of such samples provides strong protection against overfitting.

Method	Error
S-RNN ordered trees	7.18 °C
S-RNN unordered trees	6.15 °C
TreeESN M	2.78 °C
TreeESN R	8.09 °C

Table 4: Average predictive error on the tree regression task.

References

- Alvarez-Melis, David and Jaakkola, Tommi S. Tree-structured decoding with doubly-recurrent neural networks. November 2016.
- Balcan, Maria-Florina and Weinberger, Kilian Q. (eds.). *Proceedings of the 33rd International Conference on Machine Learning, ICML 2016, New York City, NY, USA, June 19-24, 2016*, volume 48 of *JMLR Workshop and Conference Proceedings*, 2016. JMLR.org.
- Dong, Li and Lapata, Mirella. Language to logical form with neural attention. In *Proceedings of the 54th Annual Meeting of the Association for Computational Linguistics, ACL 2016, August 7-12, 2016, Berlin, Germany, Volume 1: Long Papers*, 2016.
- Gallicchio, Claudio and Micheli, Alessio. Tree echo state networks. *Neurocomputing*, 101:319–337, 2013. doi: 10.1016/j.neucom.2012.08.017. URL <https://doi.org/10.1016/j.neucom.2012.08.017>.
- Gómez-Bombarelli, Rafael, Duvenaud, David K., Hernández-Lobato, José Miguel, Aguilera-Iparraguirre, Jorge, Hirzel, Timothy D., Adams, Ryan P., and Aspuru-Guzik, Alán. Automatic chemical design using a data-driven continuous representation of molecules. *CoRR*, abs/1610.02415, 2016.
- Goodfellow, Ian J., Pouget-Abadie, Jean, Mirza, Mehdi, Xu, Bing, Warde-Farley, David, Ozair, Sherjil, Courville, Aaron C., and Bengio, Yoshua. Generative adversarial networks. *CoRR*, abs/1406.2661, 2014.
- Graves, Alex. Generating sequences with recurrent neural networks. *CoRR*, abs/1308.0850, 2013. URL <http://arxiv.org/abs/1308.0850>.
- Hochreiter, Sepp and Schmidhuber, Jürgen. Long short-term memory. *Neural Computation*, 9(8): 1735–1780, 1997. doi: 10.1162/neco.1997.9.8.1735.
- Kingma, Diederik P. and Ba, Jimmy. Adam: A method for stochastic optimization. *CoRR*, abs/1412.6980, 2014.
- Kingma, Diederik P. and Welling, Max. Auto-encoding variational bayes. *CoRR*, abs/1312.6114, 2013.
- Kusner, Matt J., Paige, Brooks, and Hernández-Lobato, José Miguel. Grammar variational autoencoder. In Precup, Doina and Teh, Yee Whye (eds.), *Proceedings of the 34th International Conference on Machine Learning*, volume 70 of *Proceedings of Machine Learning Research*, pp. 1945–1954, International Convention Centre, Sydney, Australia, 06–11 Aug 2017. PMLR. URL <http://proceedings.mlr.press/v70/kusner17a.html>.
- Lavrac, Nada and Dzeroski, Saso. Relational data mining, 2001.
- Liu, Han, Xu, Min, Gu, Haijie, Gupta, Anupam, Lafferty, John D., and Wasserman, Larry A. Forest density estimation. *Journal of Machine Learning Research*, 12:907–951, 2011.
- Oliva, Junier B., Dubey, Kumar Avinava, Póczos, Barnabás, Xing, Eric P., and Schneider, Jeff G. Recurrent estimation of distributions. *CoRR*, abs/1705.10750, 2017.
- Rezende, Danilo Jimenez, Mohamed, Shakir, and Wierstra, Daan. Stochastic backpropagation and approximate inference in deep generative models. In *Proceedings of the 31th International Conference on Machine Learning, ICML 2014, Beijing, China, 21-26 June 2014*, pp. 1278–1286, 2014.
- Sohn, Kihyuk, Lee, Honglak, and Yan, Xinchun. Learning structured output representation using deep conditional generative models. In *Advances in Neural Information Processing Systems 28: Annual Conference on Neural Information Processing Systems 2015, December 7-12, 2015, Montreal, Quebec, Canada*, pp. 3483–3491, 2015.

- 398 Sutskever, Ilya, Vinyals, Oriol, and Le, Quoc V. Sequence to sequence learning with neural networks.
399 In Ghahramani, Z., Welling, M., Cortes, C., Lawrence, N. D., and Weinberger, K. Q. (eds.),
400 *Advances in Neural Information Processing Systems 27*, pp. 3104–3112. Curran Associates, Inc.,
401 2014a.
- 402 Sutskever, Ilya, Vinyals, Oriol, and Le, Quoc V. Sequence to sequence learning with neural networks.
403 In *Advances in Neural Information Processing Systems 27: Annual Conference on Neural Informa-*
404 *tion Processing Systems 2014, December 8-13 2014, Montreal, Quebec, Canada*, pp. 3104–3112,
405 2014b.
- 406 Uria, Benigno, Côté, Marc-Alexandre, Gregor, Karol, Murray, Iain, and Larochelle, Hugo. Neural
407 autoregressive distribution estimation. *Journal of Machine Learning Research*, 17:205:1–205:37,
408 2016.
- 409 van den Oord, Aäron, Dieleman, Sander, Zen, Heiga, Simonyan, Karen, Vinyals, Oriol, Graves, Alex,
410 Kalchbrenner, Nal, Senior, Andrew W., and Kavukcuoglu, Koray. Wavenet: A generative model
411 for raw audio. *CoRR*, abs/1609.03499, 2016.
- 412 Vinyals, Oriol, Bengio, Samy, and Kudlur, Manjunath. Order matters: Sequence to sequence for sets.
413 *CoRR*, abs/1511.06391, 2015.
- 414 Zaheer, Manzil, Kottur, Satwik, Ravanbakhsh, Siamak, Poczos, Barnabas, Salakhutdinov, Ruslan R,
415 and Smola, Alexander J. Deep sets. In Guyon, I., Luxburg, U. V., Bengio, S., Wallach, H., Fergus,
416 R., Vishwanathan, S., and Garnett, R. (eds.), *Advances in Neural Information Processing Systems*
417 *30*, pp. 3394–3404. Curran Associates, Inc., 2017.
- 418 Zhang, Xingxing, Lu, Liang, and Lapata, Mirella. Top-down tree long short-term memory networks.
419 In *NAACL HLT 2016, The 2016 Conference of the North American Chapter of the Association for*
420 *Computational Linguistics: Human Language Technologies, San Diego California, USA, June*
421 *12-17, 2016*, pp. 310–320, 2016.
- 422 Zhou, Ganbin, Luo, Ping, Cao, Rongyu, Xiao, Yijun, Lin, Fen, Chen, Bo, and He, Qing. Generative
423 neural machine for tree structures. *CoRR*, abs/1705.00321, 2017.

Algorithm 1 Sampling serializations

```

function SERIALISATION( $x, X, f, \mu$ )
   $a_{\text{sample}} \leftarrow ()$  ▷ Sampled serialisation from  $A$ .
   $s \leftarrow s_0$  ▷ Current state which is initialized to  $s_0$ .
   $A_{\text{all}} \leftarrow X^{-1}(x)$  ▷ This contains the set of candidate serialisations.
   $t \leftarrow 1$ 
  repeat
     $\mathcal{L} \leftarrow \text{PossibleElement}(t, A_{\text{all}})$  ▷ Lsit of all plausible next elements
     $a^{\text{next}} \leftarrow \text{Sample}(\mu, s, \mathcal{L})$  ▷ Sample  $\mathcal{L}$  according to  $\mu$  and  $s$ 
     $a_{\text{sample}} \leftarrow (a_{\text{sample}}, a^{\text{next}})$ 
     $s \leftarrow f(s, a^{\text{next}})$ 
     $A_{\text{all}} \leftarrow \text{UpdateList}(A_{\text{all}}, a^{\text{next}}, t)$  ▷ Remove from  $A_{\text{all}}$  serialisations
    ▷ not having  $a^{\text{next}}$  at position  $t$ .
     $t \leftarrow t + 1$ 
  until  $a^{\text{next}} = \text{eos}$  ▷ Stop at the end of the sequence.
  return  $a$ 
end function

```

Algorithm 2 Auxiliary functions.

```

function POSSIBLEELEMENT( $t, A_{\text{all}}$ )
   $\mathcal{L} \leftarrow \{\}$ 
  for all  $a \in A_{\text{all}}$  do
     $\mathcal{L} \leftarrow \mathcal{L} \cup \{a^t\}$  ▷ Add to  $\mathcal{L}$  element at position  $t$  of the sequence  $a$ .
  end for
  return  $\mathcal{L}$ 
end function

function SAMPLE( $\mu, s, \mathcal{L}$ )
   $\text{norm} \leftarrow \sum_{a^{\text{temp}} \in \mathcal{L}} \mu(a^{\text{temp}}, s)$ 
  for all  $a^{\text{temp}} \in \mathcal{L}$  do
     $P_{a^{\text{temp}}} \leftarrow \frac{\mu(a^{\text{temp}}, s)}{\text{norm}}$ 
  end for
   $a^{\text{temp}}$  is sampled with probability distribution  $P$ .
  return  $a^{\text{temp}}$ 
end function

function UPDATERLIST( $A_{\text{all}}, a^{\text{next}}, t$ )
   $A_{\text{temp}} \leftarrow \{\}$ 
  for all  $a \in A_{\text{all}}$  do
    if  $a^t = a^{\text{next}}$  then
       $A_{\text{temp}} \leftarrow A_{\text{temp}} \cup \{a\}$ 
    end if
  end for
  return  $A_{\text{temp}}$ 
end function

```

425 **B Detailed description of experiments and results**426 **B.1 Multivariate dynamical systems datasets**427 **B.1.1 Data structure of multivariate dynamical systems**

428 We explore the performance of S-RNN on two datasets arising from multivariate dynamical systems
 429 (artificial and real-world). We generate the artificial dataset using a known dynamical system. The real
 430 world dataset contains recordings of gait trajectories (joint angle values) of people with pathological
 431 gait. Both datasets have a similar structure and differ only by their dimensionalities and cardinalities.
 432 In particular every training instance consists of two components: $\mathbf{x} \in \mathbb{R}^d$, which we call input, and
 433 $\mathbf{Y} \in \mathbb{R}^{k \times l}$ which we call output; with the latter being a probabilistic function of the former. We will
 434 denote the i, j element of \mathbf{Y} by y_{ij} , the j column by $y_{\cdot j}$ and the i row by $y_{i \cdot}$; functions $l(y_{i \cdot})$ and
 435 $l(x_i)$ return the name of the feature they take as argument. The \mathbf{Y} matrix contains a k -dimensional
 436 dynamical system uniformly sampled at T time points. We solve two types of tasks. A supervised
 437 task in which the goal is to learn the conditional density $P(\mathbf{Y}|\mathbf{x})$ and use that for sampling and
 438 prediction and an unsupervised task in which we seek to learn $P(\mathbf{Y})$ and sample from it. In both
 439 cases we measure performance with the negative log-likelihood.

440 **B.1.2 Serialisation of multivariate dynamical systems**

441 We now describe the concrete serialisation structure that the serialization algorithm produces for a
 442 particular \mathbf{Y} matrix and a \mathbf{x}, \mathbf{Y} , couple. Our dictionary \mathbb{B} contains two types of elements, categorical

and real valued. The domain of the categorical elements is $\{l(x_i)|i := 1\dots d\} \cup \{l(y_i)|i := 1\dots k\} \cup \{t+\}$, i.e. the names of the features of the \mathbf{x} and \mathbf{Y} components and $t+$; the latter denotes a shift from a column of the \mathbf{Y} matrix to the next one, essentially it corresponds to moving to the next element of a multi-variate sequence. The real valued elements are the values of the features. Within a serialisation a categorical element is always coupled by a real value. A feature name is coupled by the respective feature value and $t+$ is always coupled with zero. The categorical elements are encoded with a one-hot vector.

When serialising matrix \mathbf{Y} and currently at column j the serialization algorithm randomly chooses among the features that have not yet been added which one to add. Thus μ is uniform over the non-selected features. Once all features of the j column have been sampled then the $t+$ operator is selected as the next element of the serialisation, and the serialization algorithm proceeds with the serialisation of the next sequence element. When we serialise an (\mathbf{x}, \mathbf{Y}) couple the sampling measure μ is now different. In half of the cases we first select all elements of the \mathbf{x} component to be added to the serialisation before moving to the serialisation of the \mathbf{Y} component. In the other half sampling between the \mathbf{x} and \mathbf{Y} components is uniform, i.e. \mathbf{x} and \mathbf{Y} features can be interleaved. Nevertheless the serialisation order of \mathbf{Y} is the same as before. We bias serialisation towards selecting first the \mathbf{x} components because we want to sample and learn the conditional distribution $P(\mathbf{Y}|\mathbf{x})$ thus the conditioning component should appear first in the serialisation. However, we still allow for a uniform sampling between the \mathbf{x} and \mathbf{Y} components in half of the cases so that the learner will have more chance to pick up on correlations between parts of the input and parts of the output. All serialisations are generated on the fly during training.

B.1.3 Learning architecture for multivariate dynamical systems

We describe the learning architectures we use. Note that these architectures are essentially the same for the baseline learning algorithms (against which we will compare) and our algorithm S-RNN. The architectural differences are only the result of the structure of the training data. In the case of the baseline algorithms these are either standard vectorial data, i.e. here the \mathbf{x} component, or a k -dimensional sequence, i.e. the \mathbf{Y} component. In the case of S-RNN the training data are the serialisations/sequences produced from a given training instance \mathbf{Y} or (\mathbf{x}, \mathbf{Y}) , where each serialisation element is a couple with a categorical component and its respective real value.

We first describe the baseline architecture. We model the probability of the next k -dimensional element in a sequence given the current state as a m -component mixture of Gaussians the parameters of which we learn. Both for the unsupervised and supervised case the core architectural element is a multivariate LSTM. For the unsupervised setting we use a two-layer LSTM (Hochreiter & Schmidhuber (1997)), with 128/256 units in each layer for the artificial/gait datasets respectively, followed by a one hidden layer neural network with 128/64 units for the artificial/gait datasets respectively. The network is fed sequentially with the k -dimensional sequence of the \mathbf{Y} matrix and predicts the means, covariance matrices, and mixture weights of the Gaussian mixture (thus its output is of dimensionality $m \times (k + k \times k) + m$), which provides the conditional distribution of the next sequence element. For the artificial data the mixture has only 1 Gaussian component and for the gait data it has 6. For the supervised setting we use an encoder-decoder architecture built on top of the architecture we just described (Sutskever et al. (2014a)). The encoder part has the same architecture as the two-layer LSTM we just described and is fed with the \mathbf{x} component, i.e. a single element sequence. The hidden states and cell states of the two layer encoder are fed to the respective states of the decoder which itself also has the same two layer architecture and as in the unsupervised case feeds to a single layer neural network. All dimensionalities are the same as before.

For S-RNN since each element of the serialisation has a categorical component and a continuous one we need to adapt the learning architecture for that structure. We use exactly the same architecture for the supervised and unsupervised experiments since there is no change in the serialisation structure between the two experiments. To adapt the baseline architecture we described in the previous paragraph to the particularities of the serialisation structure we add one more one hidden layer neural network which is fed by the output of the two-layer LSTM and together with a soft-max layer model the conditional probability of the categorical part of the next element in the serialisation. The continuous component is predicted using the same architecture as the one we describe before to predict the k -dimensional element of a sequence, with the only difference that since it is a scalar the output of the network will have $m \times (1 + 1) + m$ outputs predicting the mean, variance and mixture weights of the m component Gaussian mixture.

We optimize all architectures using Adam (Kingma & Ba (2014)). We use a mini-batch size of 32 instances for the baseline methods. In the case of S-RNN a mini-batch contains 64 serialisations which are generated from 32 instances.

B.2 Artificial dynamical system

We use a couple of Van der Pol equations linked to an harmonic oscillator to generate the artificial dynamical system. The coupling creates correlations between the variables which the learning process needs to learn. Here the dimensionality d of \mathbf{x} is 9, and the dimensionality of \mathbf{Y} is 3×21 . Given an input \mathbf{x} , its matrix \mathbf{Y} is generated by:

$$\begin{aligned}\frac{d^2 y_1(t)}{dt^2} &= -|k|_+ y_1(t) \\ \frac{d^2 y_2(t)}{dt^2} &= |\mu_y|_+ (1 - y_2(t)^2) \frac{dy_2(t)}{dt} - y_2(t) - y_1(t) \\ \frac{d^2 y_3(t)}{dt^2} &= |\mu_{y_3}|_+ (1 - y_3(t)^2) \frac{dy_3(t)}{dt} - y_3(t) - y_2(t)\end{aligned}$$

The input vector \mathbf{x} contains the initial conditions of the dynamical system and the values of its parameters, $y_1(0), y_2(0), y_3(0), \dot{y}_1(0), \dot{y}_2(0), \dot{y}_3(0), k - 3, \mu_{y_2} - 3$ and $\mu_{y_3} - 3$. These are generated randomly for each (\mathbf{x}, \mathbf{Y}) pair. We generated 3000 instances of length 21 which we divided equally to training, validation, and testing sets. We train for 12 hours or until the validation error becomes larger than the validation error of the first iteration, which in the case of the baseline happens very often. We then select the model with the lowest validation error and apply it on the test set to compute the conditional negative log-likelihood. With the artificial dynamical system we only experiment in the supervised setting; the predicted \mathbf{Y} component is the one that maximizes the $P(\mathbf{Y}|\mathbf{x})$ conditional likelihood.

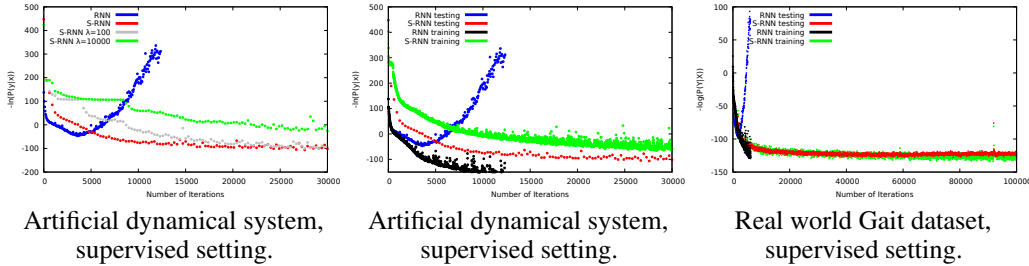


Figure 2: Overfitting behavior on the dynamical system problems, supervised setting. Left: Conditional negative log likelihood on the validation set as a function of training iterations, artificial dynamical system, includes different regularisation levels for S-RNN. Middle: Same as the left but on train/test sets. Right: Same as the middle but on the Gait dataset.

In the left part of figure 2 we give the evolution of the conditional log-likelihood on the validation as a function of the training iterations (number of mini-batches seen). The most striking observation is that S-RNN never overfits; this is even more clearly demonstrated in the middle graph of the same figure where we give the evolution of the likelihood on the train and test set for both S-RNN and RNN. The standard RNN starts overfitting after around 5k mini-batch iterations, time by which it will have seen every training instance on average 160 times. S-RNN practically will never see an instance twice due the combinatorial complexity of the serialisation generation and can keep on training practically forever and no overfitting. As we can see in Table 5 S-RNN with no regularisation achieves the best result, far better and significantly better than the baseline; we controlled the statistical significance using a t-test. Mildly regularising S-RNN does not seem to bring any performance gain, while strong regularisation harms. The fact that regularisation does not bring any effect can be explained by the fact that the algorithm never sees twice the same serialisation and thus there is no overfitting problem.

In order to inspect the visual quality of the predictive results we give in figure 3 for a given \mathbf{x} component the three components of the output sequence which has the maximum conditional probability $P(y_1|\mathbf{x})$ for RNN and S-RNN. As it is obvious S-RNN produces sequences of better quality, closer to the real sequence. serialization algorithm has different predictions as a function of the different serialisations of the \mathbf{x} component.

S-RNN	S-RNN $\lambda = 10^2$	S-RNN $\lambda = 10^4$	RNN
-107	-103	-57	-41

Table 5: Test set negative log likelihood, artificial dynamical system, supervised setting. Bold indicate performances that are significantly better than the non-bold.

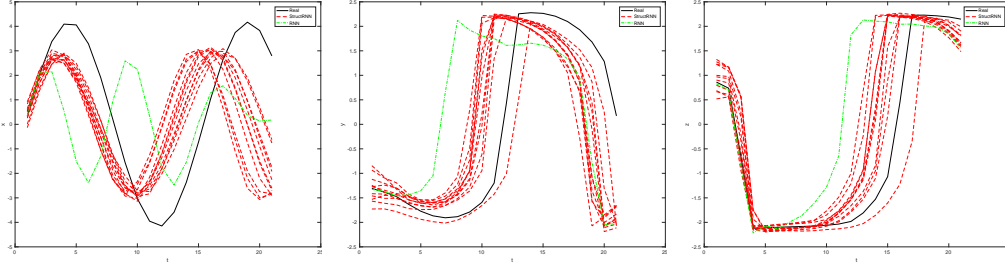


Figure 3: Examples of the y_1, y_2, y_3 sequences produced by S-RNN, RNN for the simulated dynamical system given the x component. The black curves are the real data, green is the sequence produced by RNN, and red are the sequences produced by S-RNN for different serialisations of x input.

B.3 Gait data

The gait dataset contains data for 806 patients. Every patient has an x component which is a 212-dimensional vector describing clinical properties of the patient, related to their body geometry and articulation flexibility. The Y component is an 8-dimensional sequence with 34 observations. The sequence describes a complete gait cycle of the patient, uniformly sampled at 34 points. Each one of the dimensions is an angular measurement on a joint of the patient. For each patient we have on average 6 gait cycles, giving a total of 4680 cycles. We decided to define learning instances on the level of cycles, thus we have a total of 4608 instances, all of which have an x and Y . As a result patients can appear multiple times (depending on how many cycles they have), their x component is always the same. When dividing in training, validation and testing sets, we took care to put all instances of a given patient only in one of the three sets. The training set contains 408 patients and their 3276 cycles, the validation set contains 16 patients and 1404 cycles, and the testing 382 patients and 1404 cycles. The stopping rule is the same as in the artificial dynamical system.

We first report the results on the unsupervised setting in which our goal is to learning a model of $P(Y)$. In table 6 we give the negative log-likelihood on the test set for different dimensionalities of the gait sequence. As it is clear S-RNN achieves a performance which is always considerably better than the RNN baseline. In figure 4 we give examples of samples generated from S-RNN, RNN and real gait cycles respectively. Although the graphs are not conclusive it seems that S-RNN preserves more of the real gait cycle structure, while the ones generated from RNN seem to have a more random structure.

In the supervised setting we experimented with one and two angles. This time when it comes to one angle S-RNN is significantly worse compared to RNN. The situation is reversed when we consider two angles. We hypothesize that the low performance in the one-angle setting is because most of the network representation power is consumed in learning and expressing correlations between the input features. With two angles we are able to learn and express correlations between the angles themselves, thus the better performance.

# of Angles	S-RNN mean	RNN mean
2	-6.8	7.3
4	-66	-14
8	-32	83.3

Table 6: Test set negative log likelihood on the unsupervised Gait problem. Bold indicate performances that are significantly better than non-bold.

Angles	S-RNN $\lambda = 0$	S-RNN $\lambda = 100$		S-RNN $\lambda = 10000$		RNN	
	mean	mean	p-value	mean	p-value	mean	p-value
1	-47	-44	$2 \cdot 10^{-5}$	-49	1.0	-53	1
2	-125	-114	0	-100	0	-97	0

Table 7: Test negative log likelihood on the supervised Gait problem. Bold indicate the lowest statistically significant better negative log likelihood using a t -test.

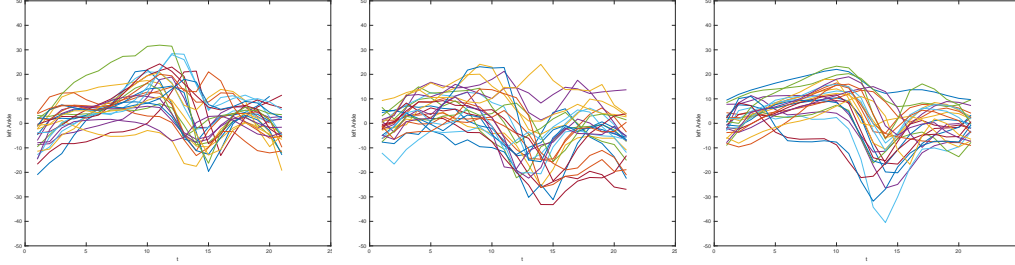


Figure 4: Left graph: Samples from S-RNN for the unsupervised Gait problem. Middle graph: Samples from RNN for the unsupervised Gait problem. Right graph: Real gait samples.

As with the artificial dataset we also check the behavior of S-RNN on the two angle dataset with respect to overfitting by visualising the evolution of the negative log likelihood in the training and testing set as a function of the number of learning iterations (number of mini-batches seen), right graph in figure 2. As it was also the case with the artificial dataset we never observe a divergence between the performance on the training and the testing set, in fact here we even S-RNN train for 100k iterations, point to which we stopped without observing any divergence between the two losses. When it come to RNN the overfitting is very severe and happens again around 5k iterations.

To visualise the quality of predictions and how they are affected by the serialisation of \mathbf{x} which we need to feed to S-RNN in order to generate the \mathbf{Y} component we give in the left part of figure 5 the different predictions we get for one angle and the different permutations of the \mathbf{x} vector. As we can see the predicted gait curves are globally consistent and rather similar to the true gait curve. Finally in right part of figure 5 we give the multiple gait cycles of a single patient, the different predictions produced by S-RNN using different serialisations of \mathbf{x} and the prediction produced by RNN. Again it is clear that the predictions generated by S-RNN are much more consistent to the true gait structure compared to the ones generated by RNN, which is considerably off from the true data structure.

B.4 Tree datasets

B.4.1 Data structures in tree datasets

We experiment with S-RNN on two different learning tasks involving instances that are represented as trees. We consider ordered and unordered trees. In the former the order of the child nodes is not important while in the latter it is. Ordered trees are mostly used in NLP tasks while unordered are used in graph modeling. The first task is a tree prediction task in which the goal is to generate a tree given a textual description of it. Thus here a learning instance is a \mathbf{x}, \mathbf{Y} , pair where the predictive component \mathbf{x} is a sequence and the target \mathbf{Y} is a tree. The second task is a regression task where the goal is to predict a scalar given a tree, i.e. learning instances are now of the form \mathbf{X}, y , where \mathbf{X} is a tree and $y \in \mathbb{R}$. As is customary in (generative) tree modeling we make the assumption that the probability distribution that governs the generation of a given node is a function of its parent nodes and its so-far seen siblings. For the tree prediction task we use the synthetic data and the evaluation code of Alvarez-Melis & Jaakkola (2016). The goal is to predict the topology of an ordered tree given only its nodes sequence as this is produced by a depth first traversal of the tree and no topological information. Node labels are taken from the 26-letter alphabet $T_1 = \{A, B, \dots, X, Y, Z\}$. We use the train/validation/test set separation of the original paper, i.e. 4000 training, 500 validation, and 500 testing instances. The tree sizes vary considerably with the smallest trees having only a single node and the largest ones 20, with the average number of nodes being 4. For the regression task the goal is to predict the

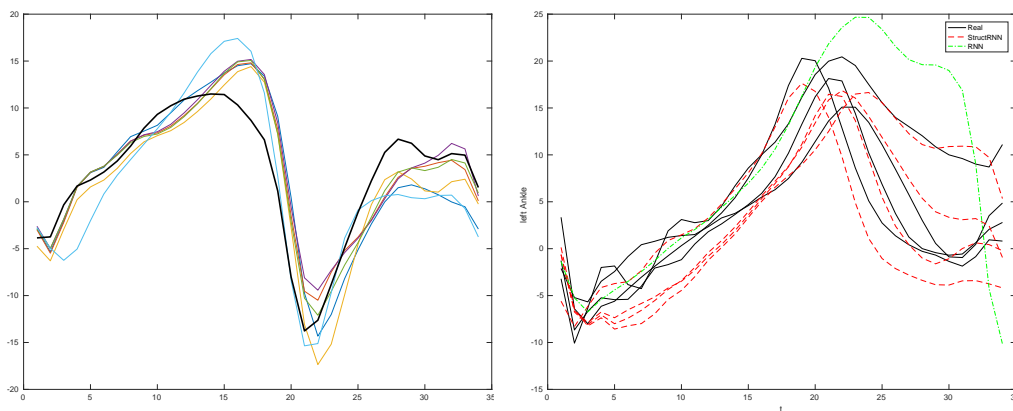


Figure 5: Left graph: Sensitivity of output prediction to the serialisation order of \mathbf{x} . The thick black curve is the real gait, the other curves are the ones generated from different perturbations of the \mathbf{x} input. Right graph: Multiple gait cycles of a given patient (black), S-RNN predictions generated from different serialisations of the \mathbf{x} of the given patient (red) and the RNN prediction (green).

boiling point of alkane molecules (Gallicchio & Micheli (2013)). Here we consider both ordered and unordered trees. The node labels are taken from the set of $T_2 = \{C, CH, CH_2, CH_3, CH_3F, CH_4\}$ where each label indicates how many hydrogen atoms are linked to the carbon atom. Here the number of nodes per tree vary from one to ten, with an average of five. The dataset has 150 learning instances. We estimate the performance by averaging the performance estimates over three hold-out sets, where the size of the hold out is 20. From the remaining 130 instances we use 100 for training and the remaining 30 for parameter tuning.

B.4.2 Serialisation for tree problems

We now describe how the serialization algorithm treats the learning instances, i.e. the (\mathbf{x}, \mathbf{Y}) or (\mathbf{X}, y) pairs, starting by describing the serialisation of a tree. In serialising tree structures the dictionary \mathbb{B} contains only categorical elements, and in particular it is the set $\{(\cdot, \cdot)\} \cup NL$, where a (\cdot, \cdot) indicates that the next element of the serialisation will be the children of the current node, \cdot indicates that we have completed the list of children of the current node, NL is the set of all node labels for the given tree problem, i.e. T_1 for the tree prediction problem and T_2 for the boiling point prediction problem. To produce the serialisation we traverse the tree in a depth first manner and add elements to the serialisation as we move from node to node. For ordered trees the order of traversal of the children of a node is the same as the one given by the tree, i.e. there is no randomness here. For unordered trees the order of traversal is random, i.e. μ is uniform over the non-selected children. To give an example, for the ordered tree with root A and two child nodes B and C its unique serialisation will be $[A, (\cdot, B, C, \cdot)]$. If the tree is unordered then it will have two possible serialisations $[A, (\cdot, B, C, \cdot)]$ and $[A, (\cdot, C, B, \cdot)]$. The state s associated with the given partial serialisation we generate just before arriving at some node, k , of a tree will be given by the sequence of the parent nodes of k and its so far-seen siblings, i.e. it does not depend on the children of its seen siblings. This state representation reflects the main assumption in tree modeling, mentioned above, i.e. that the generative distribution of a node is a function of only its parent nodes and its so-far seen siblings. We only use this state representations when we want to impose the structural constraints regulariser. The tree serialisation is one component of the learning instance serialisation. In the tree prediction problem we need to serialise (\mathbf{x}, \mathbf{Y}) pairs, where \mathbf{x} is the node label sequence of the depth-first tree traversal. Since here \mathbf{x} is already a sequence there is no serialisation involved for it. In addition since the elements come from T_1 we do not even need to extend the dictionary \mathbb{B} since the node labels will be already in. However we prefer to use a different label set, T'_1 , for the elements of the input sequences in order not to provide to the algorithm the domain knowledge about the correspondence of the building blocks of the sequences and the trees. This makes the problem more difficult since the algorithm will now need to learn these correspondences. Thus the final dictionary is $\mathbb{B} = \{(\cdot, \cdot)\} \cup T_1 \cup T'_1$. The

sampling measure μ we use to serialise a (\mathbf{x}, \mathbf{Y}) learning instance randomly selects to include first in the serialisation the \mathbf{x} component half of the times while the other half it first serialises the tree \mathbf{Y} . Essentially we are feeding the model with samples from both $P(\mathbf{Y}|\mathbf{x})$ and $P(\mathbf{x}|\mathbf{Y})$ distributions and the learning algorithm learns associations between their individual building blocks, learning eventually the complete joint distribution $P(\mathbf{x}, \mathbf{Y})$. For the regression task where the learning instances come in the form \mathbf{X}, y the dictionary is now given by $\mathbb{B} = \{(\cdot, \cdot)\} \cup \mathbf{T}_1 \cup \mathbf{t} \cup \mathbb{R}$. It thus includes also real value elements, since these are used for the target variable. The label \mathbf{t} stands for target and it will always be followed by a scalar, describing thus the target value y for the given training instance. As in the tree prediction problem the sampling measure μ selects randomly in half the serialisations the \mathbf{X} component first and in the other half the y component.

B.4.3 Learning architecture for tree problems

On the tree prediction task we compare our method against DRNN introduced in Alvarez-Melis & Jaakkola (2016) using the authors' code and their evaluation protocol. DRNN use two different hidden state vectors a fraternal and an ancestral. The fraternal hidden-state models the evolution of the state with siblings and the ancestral models the relation between parent and child. This relation is modeled with two types recurrence: one between parent and child, and one between siblings. The hidden state is then used to predict the topological information (if we grow a new branch) and the label information. The evaluation protocol treats the task as a retrieval problem quantifying the quality of the recovery of the nodes and edges of the original tree. We use the same learning architecture as the one described in B.1 with small differences in the number of hidden units and layers. Concretely we use a two-layer LSTM with 512 units followed by a two-hidden layer network that predicts the categorical component and another two hidden layer that predicts the parameters (means, variances and mixture coefficients) of 6 Gaussian mixtures. In the two latter networks the number of hidden units is tuned on the validation set from $2^i : i = 5 \dots 10$. The λ parameter of the structural constraints regulariser is also tuned from the set $(0, 1, 10, 100)$. We report choose the best model on the validation set and report the testing error. As before we use ADAM for optimization. We use a mini-batch size of 32 instances for DRNN. For S-RNN a mini-batch contains 64 serialisations which are generated from 32 instances.

B.4.4 Tree results

We give the results in table 8. S-RNN outperforms DRNN by a large margin, a method specifically developed to learn with trees, both for the F1 and precision measures for nodes and edges. It fails worse for node and edge recall. DRNN has a perfect recall, at the cost of generating trees which have many superfluous elements.

Method	Node F1	Node precision	Node Recall	Edge F1	Edge Precision	Edge Recall
S-RNN	88.95%	87.82%	90.79%	83.43%	82.22%	85.47%
DRNN	74.51%	59.37%	100%	65.86%	49.10%	100%

Table 8: Performance results for the tree prediction task.

In the regression task of predicting a scalar given a tree we compare S-RNN against two variants Tree Echo State Network, TreeESN-R and TreeESN-M, Gallicchio & Micheli (2013). Both TreeESN methods are reservoir computing models which generalize the reservoir computing paradigm to tree structured data. The difference between the two variants is on how they aggregate the state vectors to represent the complete tree. The R variant only use the state of the root whereas the M variant averages over all states of the tree. We formulate the problem as both learning with ordered and unordered trees. The evaluation error is the mean absolute error. We give the performance results in table 9 (average predictive error). The two variants of S-RNN, i.e. trained on ordered and unordered trees, give better results than TreeESN-R, while they perform worse than TreeESN-M. The performance of all methods is quite remarkable given that the scalar values to predict range from -164°C to 174°C .

In order to check the behavior of S-RNN with respect to overfitting we also plot the evolution of the loss function in the train/validation/test sets in figure 6. When it comes to the tree prediction task and the tree regression task with the unordered trees there is hardly any divergence between the losses

Method	Error
S-RNN ordered trees	7.18 °C
S-RNN unordered trees	6.15 °C
TreeESN M	2.78 °C
TreeESN R	8.09 °C

Table 9: Average predictive error on the tree regression task.

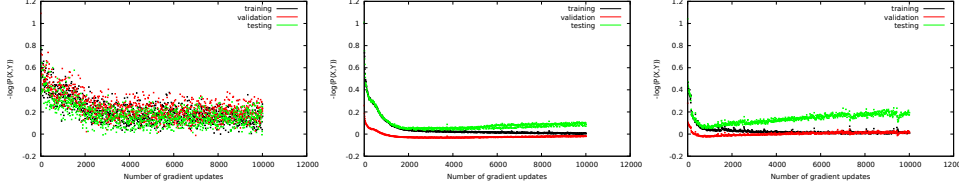


Figure 6: Evolution of loss in training/validation/test sets with the number of gradient updates for the tree problems: tree prediction task (left), tree regression, ordered trees, (middle), tree regression, unordered trees, (right).

673 computed over the three different datasets. In the case of ordered trees we do observe an important
674 divergence starting from around the 2000th gradient update. In serialising an ordered tree there is no
675 randomness since you respect the order, thus an ordered tree has a single serialisation, contrary to the
676 ordered ones which have multiple serialisations. Exposing the learning algorithm to multiple random,
677 but equivalent, serialisations provides clear benefits in terms of protection against overfitting.

678 B.5 Propositional datasets

679 We also explore the performance of S-RNN on a set of standard propositional classification datasets
680 taken from the UCI repository. These datasets have a mix of d_n numeric and d_c categorical attributes.
681 Given a training instance \mathbf{x} we will use $\mathbf{x}^{d_n} \in \mathbb{R}^{d_n}$ to denote the vector of its numerical components
682 and $\mathbf{x}^{d_c} \in \mathbb{N}^{d_c}$ to denote the vector of its categorical components. We denote by y the label of \mathbf{x} , and
683 $y \in \mathbb{Y} = \{1, \dots, c\}$. We use S-RNN to learn the joint probability $P(\mathbf{x}, y)$ which we use to classify
684 instances according to the $\arg \max_y P(y|\mathbf{x})$ rule. We evaluate the performance using predictive
685 accuracy.

686 B.5.1 Serialisation of propositional instances

687 We now describe the serialisation structure that the serialization algorithm produces for a particular
688 learning instance (\mathbf{x}, y) . Our dictionary \mathbb{B} contains real-valued and categorical elements. The domain
689 of the categorical elements is the set of the feature names together with the set of values of all the
690 categorical attributes. Thus $\mathbb{B} = \{l(x_i^{d_n}) | i := 1 \dots d_n\} \cup \{l(x_i^{d_c}) | i := 1 \dots d_c\} \cup l(y) \cup \mathbb{Y} \cup \mathbb{R}$. One
691 should pay attention that every feature name and value of discrete features have a unique name.
692 As before $l(x_i)$ is a function which returns the name x_i feature. Within a serialisation a numerical
693 feature name is always coupled by its respective value, while a categorical feature name is always
694 coupled with zero. The categorical elements of the dictionary are encoded as one-hot vectors. To
695 serialise an instance the serialiser selects randomly, among its features that are not yet included in its
696 serialisation, the next one for inclusion. To describe the state s of a partial serialisation of learning
697 instance (\mathbf{x}, y) we use the set of $(l(x_i), x_i), (l(y), y)$, i.e. feature names and their values, that have
698 been so far included in the serialisation. It is easy to check equality between partial serializations
699 in order to use it within the structural constraint regulariser, by checking a set equality over the
700 respective state representations.

701 B.5.2 Learning architectures for propositional instances

702 We compare S-RNN against a standard Multilayer Neural Network baseline trained using the cross
703 entropy loss. We tune the architecture of the baseline by doing a grid search to select the number of
704 layers from (1,2,3) and the number of hidden units from (32,64,128,256). For S-RNN we use the
705 same learning architecture as the one described in B.1 with small modifications in the number of

Dataset	# Training instances	# Testing instances	#features	#Classes	S-RNN	MLP
German	686	250	20	2	75%	78%
Image	210	2038	19	7	93%	88%
Iris	75	50	4	3	99%	99%
Pendigits	7494	3498	16	10	89%	89%

Table 10: Predictive accuracy for the propositional classification datasets.

layers and hidden units. We use a two-layer and 256 unit LSTM and we use the same range of values as our baseline to determine the number of the hidden units for the neural-network that computes the mean, covariance matrix and mixture components. The regularisation parameter λ is selected from (0,1,10,100). The number of mixture components is 6. We train with early stopping on the validation set. We evaluate the predictive accuracy on a hold-out test set whenever this is available (images, pendigits); if a hold-out test set is not available then we use one third of the instances as hold out. The validation set is one sixth of the total instance number when no hold-out set was given; when a hold-out set is given you remove one quarter and use it for validation set. The detailed training and testing sizes, together with a short description of the datasets is given in table 10. As before we use ADAM to optimize, with a mini batch of size 32 for the baseline, and a mini batch size of 64 instances generated from 32 real instances by generating two serialisations for each one of them for S-RNN.

B.5.3 Results for propositional problems

We give the evaluation results in table 10. S-RNN has a performance that is similar to the MLP baseline. The reason is that for such simple tasks our model does not have any additional information that it can use, compared to the information available to the standard baseline.

Once again we remark the resistance of S-RNN to overfitting. We give in figure 7 the evolution of the log-likelihood and the cross-entropy loss on the training/validation/test sets for S-RNN and the MLP baseline, respectively, for all propositional datasets. We rescaled the y -axis into [0,1] for both losses for comparability. As we can see, the divergence of the three losses for the S-RNN is very small (with the exception of iris), even after 6000 training iterations. In fact in the German and pendigits datasets we never observed a divergence up to the 10k training iterations that we let S-RNN run for. We believe that the overfitting protection does not kick-in for iris due to the very small number of features (only four) which means that there is not enough diversity in the generated serialisations; a set of 4 features has only 24 reorderings. On the other hand the MLP baseline shows large to very large divergences between the training/validation/test set losses, and this rather early in the training iterations (2k training steps or even earlier).

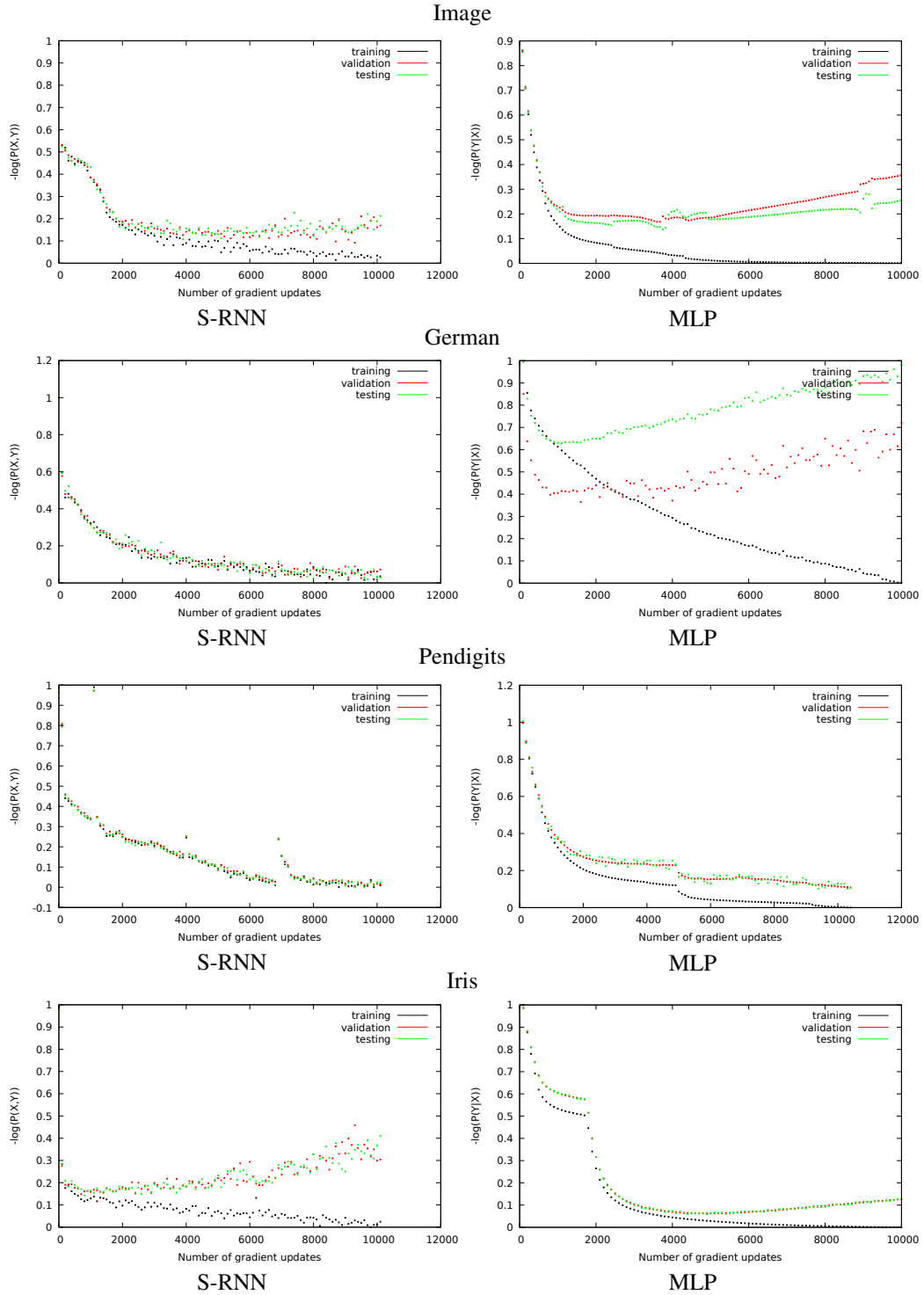


Figure 7: Evolution of the conditional negative log-likelihood loss and cross-entropy in training/validation/test sets as a function of the training iterations for S-RNN (left) and the MLP baseline (right) respectively.